Production of large transverse momentum dileptons and photons in pp, dA, and AA collisions by photoproduction processes

Yong-Ping Fu and Yun-De Li
Department of Physics, Yunnan University, Kunming 650091, China
(Received 8 July 2011; revised manuscript received 14 September 2011; published 19 October 2011)

The production of large P_T dileptons and photons originating from photoproduction processes in pp, dA, and AA collisions is calculated. We find that the contribution of dileptons and photons produced by photoproduction processes is not prominent at Relativistic Heavy Ion Collider (RHIC) energies. However, the numerical results indicate that the modification of photoproduction processes becomes evident in the large P_T region for pp, dA and AA collisions at Large Hadron Collider (LHC) energies.

DOI: 10.1103/PhysRevC.84.044906 PACS number(s): 12.39.St, 13.85.Qk, 25.75.−q, 12.38.Mh

I. INTRODUCTION

Hadronic processes for producing large transverse momentum (P_T) dileptons and photons are very important in the research of relativistic pp, dA, and AA collisions. Since photons and dileptons do not participate in the strong interaction directly, the photon or dilepton production can test the predictions of pQCD calculations, and probe the strong interacting matter (quark-gluon plasma, QGP). The hard scattering of partons is a well-known source of large P_T dileptons and photons in relativistic hadronic collisions. The photons (and dileptons) are produced from various processes in relativistic AA collisions (relativistic heavy ion collisions): primary hard photons from initial parton collisions [1–11], thermal photons from the QGP [12–21], and hadronic gas [22–26], photons from the jet-photon conversion in the thermal medium [27–30], and photons from hadronic decays after freeze-out [31]. In relativistic AA collisions the contribution of photons produced by the jet-photon conversion in the thermal medium is also important in the large P_T region [27,28].

In the present work, we investigate the production of large P_T dileptons and photons induced by photoproduction processes in pp, dA, and AA collisions at Relativistic Heavy Ion Collider (RHIC) and Large Hadron Collider (LHC) energies. The photoproduction processes play a fundamental role in the ep deep inelastic scattering at Hadron Electron Ring Accelerator (HERA) [32–35]. In photoproduction processes of the ep deep inelastic scattering, a high energy photon emitted from the incident electron directly interacts with the proton by the interaction of $\gamma p \to$ jets. Besides, the uncertainty principle allows the high energy photon for a short time to fluctuate into a quark-antiquark pair which then interacts with the partons of the proton. In such interactions the resolved photon can be regarded as an extended object consisting of quarks and also gluons. The interactions are the so-called resolved photoproduction processes.

We extend the photoproduction mechanism to the photon and dilepton production in pp, dA, and AA collisions. Charged partons of the incident nucleon also can emit high energy photons (and resolved photons) in relativistic hadron-hadron, hadron-nucleus, and nucleus-nucleus collisions. The photon spectrum from the charged parton is given by [36,37]

$$f_{\gamma/q}(z) = e_q^2 \frac{\alpha}{2\pi} \frac{1+(1-z)^2}{z} \ln\left(\frac{Q_1^2}{Q_2^2}\right), \qquad (1)$$

where α is the electromagnetic coupling parameter, z is the momentum ratio of the photon energy and the energy of the quark, the values Q_1^2 and Q_2^2 stand for the maximum and minimum value of the momentum transfer, respectively. In direct photoproduction processes, the high energy photon emitted from the charged parton of the incident nucleon interacts with the parton of another incident nucleon by the interaction of $q\gamma \to q\gamma^*$(or γ). In resolved photoproduction processes, the hadron-like photon interacts with the parton of the nucleon by the interactions of $q_\gamma \bar{q} \to g\gamma^*$, $q_\gamma g \to q\gamma^*$, and $g_\gamma q \to q\gamma^*$, here $q_\gamma(g_\gamma)$ denotes the parton of the resolved photon.

The paper is organized as follows. In Sec. II we present the production of large P_T dileptons and photons in hadronic collisions. The direct and resolved photoproduction processes are presented. In Sec. III we briefly review the production of thermal dileptons and photons in the QGP. In Sec. IV the production rate of jet-dilepton (photon) conversion is discussed. The numerical results at RHIC and LHC energies are plotted in Sec. V. Finally, the summary is given in Sec. VI.

II. LARGE P_T DILEPTON AND PHOTON PRODUCTION

A. Large P_T dilepton production

The large P_T dileptons produced by initial parton collisions can be divided into two categories: direct dileptons produced by the annihilation and Compton scattering of partons, fragmentation dileptons produced by the bremsstrahlung emitted from final state partons [4–6]. The direct dileptons (dir.l^+l^-) produced by the subprocesses $q\bar{q} \to g(\gamma^* \to l^+l^-)$ and $qg \to q(\gamma^* \to l^+l^-)$ in the hadronic collisions($AB \to l^-l^+X$) satisfy the following invariant cross section [2,4–6]:

$$\frac{d\sigma_{\text{dir.}l^+l^-}}{dM^2dP_T^2dy} = \frac{1}{\pi}\int dx_a G_{a/A}(x_a,Q^2)G_{b/B}(x_b,Q^2) \times \frac{x_a x_b}{x_a - x_1}\frac{d\hat{\sigma}}{dM^2 d\hat{t}}(x_a,x_b,P_T,M^2), \qquad (2)$$

where the functions $G_{a/A}(x_a, Q^2)$ and $G_{b/B}(x_b, Q^2)$ are parton distributions of nucleons, x_a and x_b are the parton's momentum fraction. We have $x_b = (x_a x_2 - \tau)/(x_a - x_1)$. The variables are $x_1 = (x_T^2 + 4\tau)^{1/2} e^y/2$, $x_2 = (x_T^2 + 4\tau)^{1/2} e^{-y}/2$, $x_T = 2P_T/\sqrt{s_{NN}}$ and $\tau = M^2/s_{NN}$. y is the rapidity, M is the invariant mass of the lepton pair and $\sqrt{s_{NN}}$ is the energy of the nucleon in the center-of-mass system.

The cross section of the subprocesses $ab \to l^+l^-d$ with the invariant mass squared M^2 and Mandelstam variable $\hat{t}$ can be written as [2,4]

$$\frac{d\hat{\sigma}}{dM^2 d\hat{t}}(ab \to l^+l^-d) = \frac{\alpha}{3\pi M^2}\sqrt{1-\frac{4m_l^2}{M^2}}\left(1+\frac{2m_l^2}{M^2}\right)\frac{d\hat{\sigma}}{d\hat{t}}(ab\to\gamma^* d), \quad (3)$$

where m_l is the lepton mass. Here $d\hat{\sigma}/d\hat{t}(ab \to \gamma^* d)$ denotes the cross section of $q\bar{q} \to g\gamma^*$ and $qg \to q\gamma^*$ [2].

The parton distribution $G_{i/A}(x_i, Q^2)$ of the nucleon is given by [8]

$$G_{i/A}(x_i, Q^2) = R_{i/A}(x_i, Q^2)\left[\frac{Z}{A}p_i(x_i, Q^2) + \frac{N}{A}n_i(x_i, Q^2)\right], \quad (4)$$

where $R_{i/A}(x_i, Q^2)$ is the nuclear modification factor [11], Z is the proton number, N is the neutron number, and A is the nucleon number. $p_i(x_i, Q^2)$ and $n_i(x_i, Q^2)$ are the parton distributions of protons and neutrons, respectively. We choose the momentum scale as $Q^2 = 4P_T^2$.

The fragmentation dileptons (fra.l^+l^-) are produced by the hard scattering $ab \to (c \to xl^+l^-)d$ [2,4–6]. The invariant cross section of fragmentation dileptons is

$$\frac{d\sigma_{\text{fra}.l^+l^-}}{dM^2 dP_T^2 dy} = \frac{1}{\pi}\int dx_a \int dx_b G_{a/A}(x_a, Q^2) G_{b/B}(x_b, Q^2) \times D_{q_c}^{l^+l^-}(z_c, Q^2)\frac{x_a x_b}{z_c(x_a x_b - \tau)} \times \frac{d\hat{\sigma}_{\text{par.}}}{d\hat{t}}(x_a, x_b, z_c, P_T, M^2), \quad (5)$$

where $z_c = (x_a x_2 + x_b x_1)/(x_a x_b - \tau)$ is the momentum fraction of the final state dilepton. The dilepton fragmentation function is given by

$$D_{q_c}^{l^+l^-}(z_c, M^2, Q^2) = \frac{\alpha}{3\pi M^2}\sqrt{1-\frac{4m_l^2}{M^2}}\left(1+\frac{2m_l^2}{M^2}\right) D_{q_c}^{\gamma^*}(z_c, Q^2), \quad (6)$$

where $D_{q_c}^{\gamma^*}(z_c, Q^2)$ is the virtual photon fragmentation function [4]. $d\hat{\sigma}_{\text{par.}}/d\hat{t}$ denotes the cross section of the subprocesses. These subprocesses are $qq' \to qq'$, $q\bar{q}' \to q\bar{q}'$, $qq \to qq$, $q\bar{q} \to q'\bar{q}'$, $q\bar{q} \to q\bar{q}$, $gg \to q\bar{q}$, $qg \to qg$, $q\bar{q} \to gg$, and $gg \to gg$ [1].

B. Photoproduction processes in large P_T dilepton production

In direct photoproduction processes, the parton a of the incident nucleon A can emit a large P_T photon, then the high energy photon interacts with the parton b of another incident nucleon B by the interaction of $q_b\gamma \to q(\gamma^* \to l^+l^-)$. The invariant cross section of large P_T dileptons produced by direct photoproduction processes (dir. pho.) is given by

$$\frac{d\sigma_{\text{dir.pho.}}}{dM^2 dP_T^2 dy} = \frac{2}{\pi}\int dx_a \int dx_b G_{a/A}(x_a, Q^2) G_{b/B}(x_b, Q^2) \times f_{\gamma/q_a}(z_a)\frac{x_a x_b z_a}{x_a x_b - x_a x_2} \times \frac{d\hat{\sigma}}{dM^2 d\hat{t}}(x_a, x_b, z_a, P_T, M^2), \quad (7)$$

where $f_{\gamma/q_a}(z_a)$ is the photon spectrum from the quark. According to [37] we choose Q_1^2 to be the maximum value of the momentum transfer given by $\hat{s}/4 - m_l^2$ and the choice of the momentum transfer $Q_2^2 = 1$ GeV^2 is made such that the photon is sufficiently off shell for the parton model to be applicable. $\hat{s} = x_a x_b z_a s_{NN}$ is the square of the center-of-mass energy for the subprocesses. The function $d\hat{\sigma}/dM^2 d\hat{t}$ denotes the cross section of subprocess $q\gamma \to q(\gamma^* \to l^+l^-)$ [2]. Here

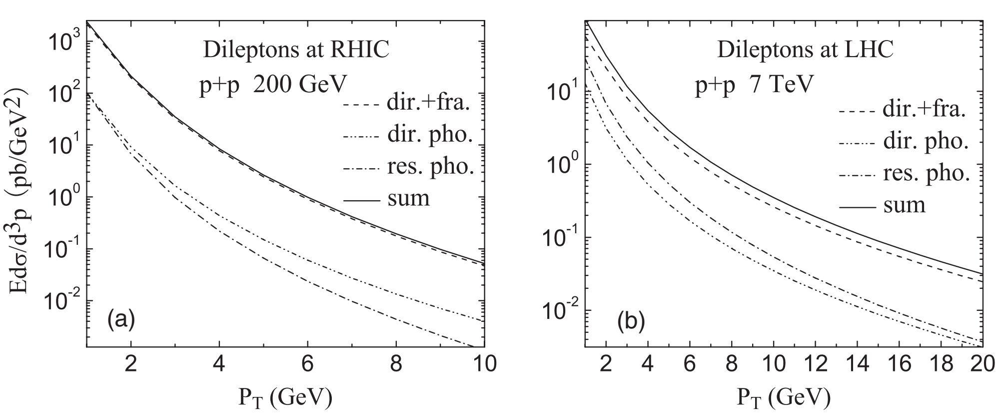

FIG. 1. (a) Invariant cross section of dileptons for $y = 0$ in $p + p$ collisions at $\sqrt{s} = 200$ GeV. Dashed line—the sum of direct dileptons (dir.) and fragmentation dileptons (fra.). Dash-dot-dot line—dileptons produced by direct photoproduction processes (dir.pho.). Dash-dot line—dileptons produced by resolved photoproduction processes (res.pho.). Solid line—the sum of direct dileptons, fragmentation dileptons, and dileptons produced by photoproduction processes. (b) Same as (a) but for $p + p$ collisions at $\sqrt{s} = 7$ TeV.

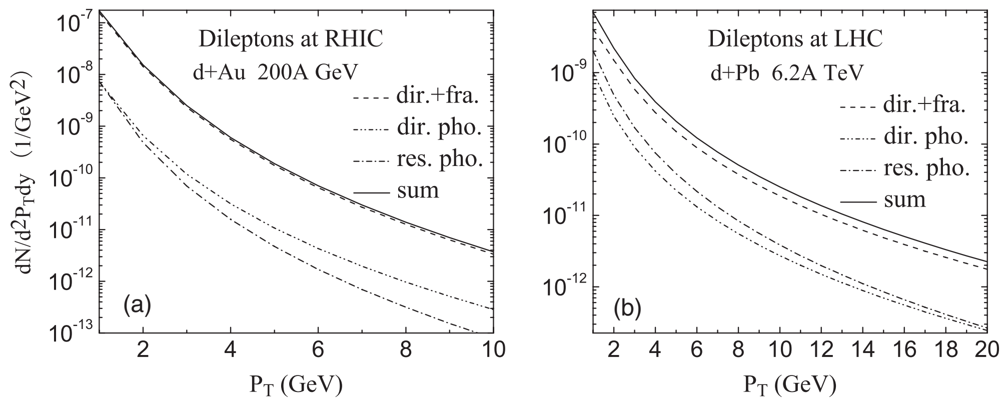

FIG. 2. Dilepton yield for $y = 0$ in central $d + \mathrm{Au}$ collisions at $\sqrt{s_{NN}}$ =200 GeV (a) and $d + \mathrm{Pb}$ collisions at $\sqrt{s_{NN}}$ =6.2 TeV (b).

$z_a = (x_b x_1 - \tau)/(x_a x_b - x_a x_2)$ is the momentum fraction of the photon emitted from the quark of the nucleon.

In resolved photoproduction processes, the parton a of the incident nucleon A emits a high energy resolved photon, then the parton a' of the resolved photon interacts with the parton b of another incident nucleon B by the interactions of $q_{a'}\bar{q}_b \to g\gamma^*$, $q_{a'}g_b \to q\gamma^*$ and $q_b g_{a'} \to q\gamma^*$. The invariant cross section of large P_T dileptons produced by resolved photoproduction processes (res. pho.) can be written as

$$\frac{d\sigma_{\text{res.pho.}}}{dM^2 dP_T^2 dy} = \frac{2}{\pi}\int dx_a \int dx_b \int dz_{a'} G_{a/A}(x_a, Q^2) \times G_{b/B}(x_b, Q^2) f_{\gamma/q_a}(z_a) G_{q_{a'}/\gamma}(z_{a'}, Q^2) \times \frac{x_a x_b z_a z_{a'}}{x_a x_b z_{a'} - x_a z_{a'} x_2} \times \frac{d\hat{\sigma}}{dM^2 d\hat{t}}(x_a, x_b, z_a, z_{a'}, P_T, M^2), \quad (8)$$

where $G_{q_{a'}/\gamma}(z_{a'}, Q^2)$ is the parton distribution of the resolved photon [10]. The cross section $d\hat{\sigma}/dM^2 d\hat{t}$ of $q\bar{q} \to g(\gamma^* \to l^+l^-)$ and $qg \to q(\gamma^* \to l^+l^-)$ is discussed in Eq. (3). The variable $z_{a'}$ denotes the momentum fraction of the parton of the resolved photon emitted from the quark. Here we have $z_a = (x_b x_1 - \tau)/(x_a x_b z_{a'} - x_a z_{a'} x_2)$ and $\hat{s} = x_a x_b z_a z_{a'} s_{NN}$.

C. Real photon production

Because a virtual photon can directly decay into a dilepton, the invariant cross sections of large P_T photons can be derived from the cross sections of the dilepton production if the invariant mass of the lepton pair is zero ($M^2 = 0$). The maximum momentum transfer Q_1^2 in Eq. (1) is $\hat{s}/4$ in the real photon production. The prompt photons are produced by the direct production (dir.γ) and the fragmentation process (fra.γ). The invariant cross section for direct photons is given by [1–3]

$$E\frac{d\sigma_{\text{dir.}\gamma}}{d^3P} = \frac{1}{\pi}\int dx_a G_{a/A}(x_a, Q^2) G_{b/B}(x_b, Q^2)\frac{x_a x_b}{x_a - x_1} \times \frac{d\hat{\sigma}}{d\hat{t}}(x_a, x_b, P_T), \quad (9)$$

where $x_b = x_a x_2/(x_a - x_1)$. In the real photon case we have $x_1 = x_T e^y/2$ and $x_2 = x_T e^{-y}/2$. The function $d\hat{\sigma}/d\hat{t}$ of

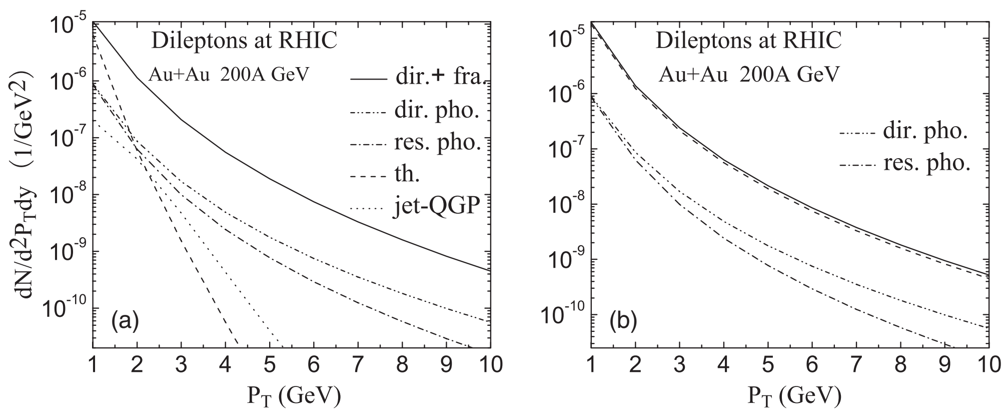

FIG. 3. (a) Dilepton yield for $y = 0$ in central Au + Au collisions at $\sqrt{s_{NN}} = 200$ GeV. Solid line—the sum of direct dileptons (dir.) and fragmentation dileptons (fra.). Dash-dot-dot line—dileptons produced by direct photoproduction processes (dir.pho.). Dash-dot line—dileptons produced by resolved photoproduction processes (res.pho.). Dash line—thermal dileptons (th.) produced by the QGP. Dot line—the jet-dilepton conversion (jet-QGP) in the plasma. (b) The contribution of photoproduction processes at RHIC energies. Dashed line—the sum of direct dileptons, fragmentation dileptons, thermal dileptons produced by the QGP and dileptons from the jet-dilepton conversion. Solid line—the sum of the dashed line, dash-dot line, and dash-dot-dot line.

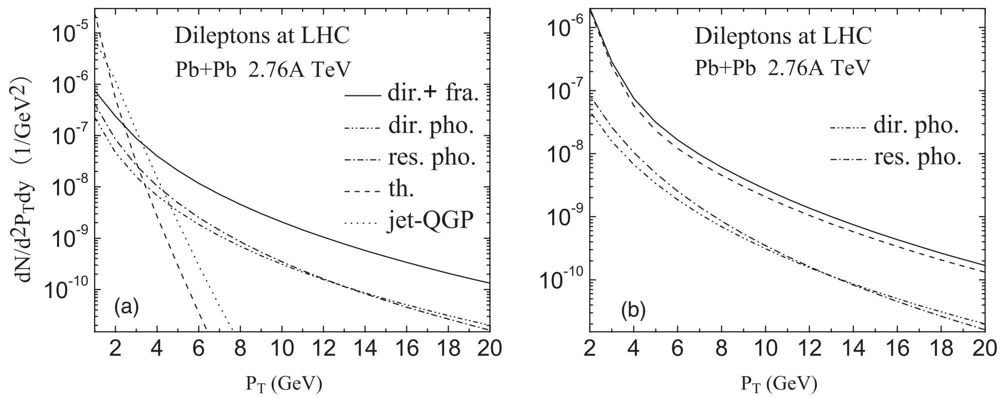

FIG. 4. Same as Fig. 3 but for central Pb + Pb collisions at $\sqrt{s_{NN}} = 2.76$ TeV.

Eq. (9) denotes the cross section of subprocesses $q\bar{q} \to g\gamma$ and $qg \to q\gamma$ [1]. The invariant cross section for fragmentation photons is given by [1–3]

$$E\frac{d\sigma_{\text{fra.}\gamma}}{d^3P} = \frac{1}{\pi}\int dx_a \int dx_b G_{a/A}(x_a, Q^2)G_{b/B}(x_b, Q^2) \times \frac{D^{\gamma}_{q_c}(z_c, Q^2)}{z_c}\frac{d\hat{\sigma}_{\text{par.}}}{d\hat{t}}(x_a, x_b, z_c, P_T), \quad (10)$$

where $D^{\gamma}_{q_c}(z_c, Q^2)$ is the real photon fragmentation function and $z_c = x_1/x_a + x_2/x_b$ [1,3]. The cross section $d\hat{\sigma}_{par.}/d\hat{t}$ of Eq. (10) is discussed in Eq. (5).

The invariant cross section of real photons produced by direct photoproduction processes is

$$E\frac{d\sigma_{\text{dir.pho.}}}{d^3P} = \frac{2}{\pi}\int dx_a \int dx_b G_{a/A}(x_a, Q^2)G_{b/B}(x_b, Q^2) \times f_{\gamma/q_a}(z_a)\frac{x_a x_b z_a}{x_a x_b - x_a x_2} \times \frac{d\hat{\sigma}}{d\hat{t}}(x_a, x_b, z_a, P_T), \quad (11)$$

where $z_a = x_b x_1/(x_a x_b - x_a x_2)$. The real photon production of resolved photoproduction processes is

$$E\frac{d\sigma_{\text{res.pho.}}}{d^3P} = \frac{2}{\pi}\int dx_a \int dx_b \int dz_{a'} G_{a/A}(x_a, Q^2) \times G_{b/B}(x_b, Q^2) f_{\gamma/q_a}(z_a) G_{q_{a'}/\gamma}(z_{a'}, Q^2) \times \frac{x_a x_b z_a z_{a'}}{x_a x_b z_{a'} - x_a z_{a'} x_2}\frac{d\hat{\sigma}}{d\hat{t}}(x_a, x_b, z_a, z_{a'}, P_T), \quad (12)$$

where the elementary cross sections $d\hat{\sigma}/d\hat{t}$ of Eqs. (11) and (12) are similar to the cases of the dilepton production in Eqs. (7) and (8) (but with $M^2 = 0$), respectively. Here we have $z_a = x_b x_1/(x_a x_b z_{a'} - x_a z_{a'} x_2)$ for Eq. (12).

III. PRODUCTION OF THERMAL DILEPTONS AND PHOTONS

The yield of thermal dileptons (th.l^+l^-) with the low dilepton mass and large transverse momentum can be written as [12,15,22]

$$\frac{dN_{\text{th.}l^+l^-}}{dM^2 dP_T^2 dy} = \pi R_A^2 \frac{\sigma_{q\bar{q}}(M)}{4(2\pi)^4} M^2 \sqrt{1 - \frac{4m_q^2}{M^2}} \frac{3\tau_0^2 T_0^6}{P_T^6} \times \left[G\left(\frac{P_T}{T_0}\right) - G\left(\frac{P_T}{T_c}\right)\right], \quad (13)$$

where R_A is the nuclear radius, m_q is the quark mass. τ_0 and T_0 are the initial time and the initial temperature of the system, respectively. We use $\tau_0 = 0.26$ fm/c for RHIC, $\tau_0 = 0.09$ fm/c for LHC ($\sqrt{s_{NN}} = 2.76$ TeV) and $\tau_0 = 0.088$ fm/c for LHC ($\sqrt{s_{NN}} = 5.5$ TeV). The initial temperature of the

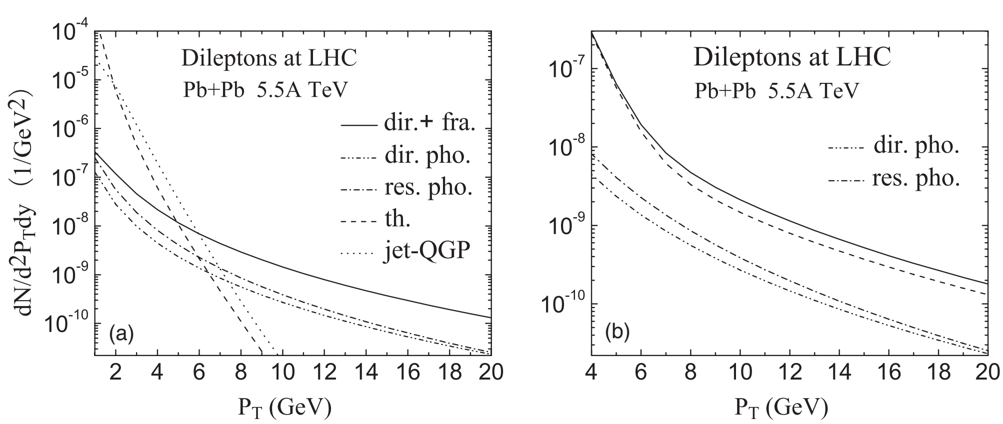

FIG. 5. Same as Fig. 3 but for central Pb + Pb collisions at $\sqrt{s_{NN}} = 5.5$ TeV.

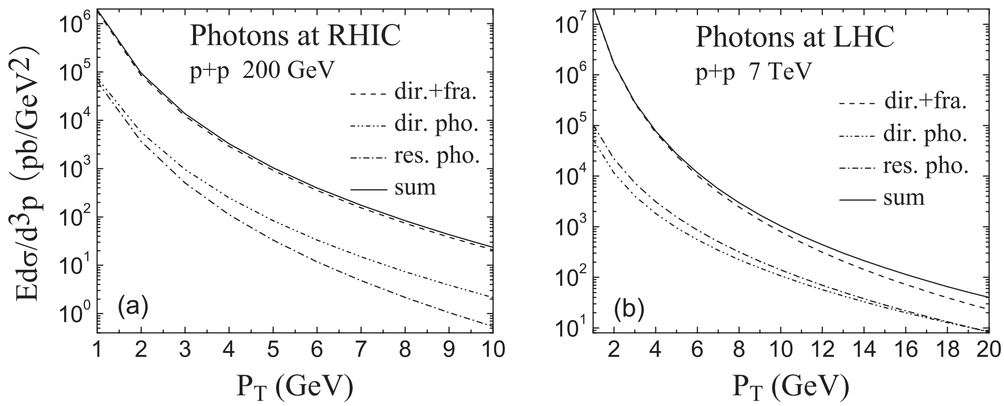

FIG. 6. Same as Fig. 1 but for the real photon production in $p + p$ collisions at RHIC (a) and LHC (b) energies.

QGP is chosen as $T_0 = 370$ MeV for Au + Au collisions at $\sqrt{s_{NN}} = 200$ GeV, $T_0 = 710$ MeV for Pb + Pb collisions at $\sqrt{s_{NN}} = 2.76$ TeV, and $T_0 = 845$ MeV for Pb + Pb collisions at $\sqrt{s_{NN}} = 5.5$ TeV. $T_c(=160$ MeV) is the critical temperature of the phase transition [3]. Here $\sigma_{q\bar{q}} = 4\pi\alpha^2 N_c N_s^2 e_q^2/3M^2$ is the cross section of the process $q\bar{q} \to \gamma^* \to l^+l^-$, $N_c(=3)$ is the color number, $N_s(=2)$ is the spin number. The function $G(z)$ is given by $G(z) = z^3(8 + z^2)K_3(z)$.

The yield of thermal photons (th.γ) is given by the following [13,15]:

$$E\frac{dN_{\text{th.}\gamma}}{d^3P} = \pi R_A^2 \frac{\alpha\alpha_s e_q^2}{4\pi^2}\int_{\tau_0}^{\tau_c} \tau d\tau f_{\text{th}}(\boldsymbol{p}_\gamma)T^2 \times \left[2\ln\left(\frac{6E_\gamma}{\pi\alpha_s T}\right) + C_{\text{Com.}} + C_{\text{ann.}}\right], \quad (14)$$

where $\tau_c = \tau_0(T_0/T_c)^3$ is the critical time of the phase transition. The parameters are $C_{\text{Com.}} = -0.416$ and $C_{\text{ann.}} = -1.916$. f_{th} is the thermal distribution of thermal partons. In the Bjorken expansion, the temperature evolves as $T = T_0(\tau_0/\tau)^{1/3}$ [14].

IV. JET-DILEPTON(PHOTON) CONVERSION

The jet-dilepton conversion is induced by the annihilation of jets passing through the QGP [38,39]. We rigorously derive the dilepton production rate of the jet-dilepton conversion. Using the relativistic kinetic theory the production rate can be written as $R_{\text{jet}-l^+l^-} \propto 1/(2\pi)^6 \int d^3\boldsymbol{p}_1 \int d^3\boldsymbol{p}_2 f(\boldsymbol{p}_1) f(\boldsymbol{p}_2) v_{12}\sigma$, where the relative velocity is $v_{12} = (p_1 + p_2)^2/2p_1^0 p_2^0$. After some algebra the rate can be written as

$$\frac{dR_{\text{jet}-l^+l^-}}{dM^2 dP_T^2} = \frac{\sigma_{q\bar{q}} M^2}{2(2\pi)^4}\int dP'_T \frac{f_{\text{jet}}(P'_T)}{4P'_T} e^{-\frac{P_T^2}{4P'_T T}}, \quad (15)$$

where f_{jet} is the phase-space distribution of jets with the large transverse momentum (P'_T). If the jet distribution is replaced by the thermal distribution $\exp(-E/T) = \exp(-P'_T \cosh y/T)$, one can obtain the rate for producing thermal dileptons.

The phase-space distribution of jets is given by [27,28]

$$f_{\text{jet}}(P'_T) = \frac{(2\pi)^3}{g\pi R_\perp^2 \tau P'_T \cosh y}\frac{dN_{\text{jet}}}{d^2P'_T dy}\delta(\eta - y) \times \Theta(\tau - \tau_i)\Theta(\tau_{\max} - \tau)\Theta(R_\perp - r), \quad (16)$$

where $g(=6)$ is the spin and color degeneracy of quarks, $R_\perp$ is the transverse radius of the system, η is the space-time rapidity of the system, τ_i is the formation time for the jet. We take $\tau_{\max}$ as the smaller of the lifetime of the QGP and the time taken by the jet produced at position r to reach the surface of the QGP.

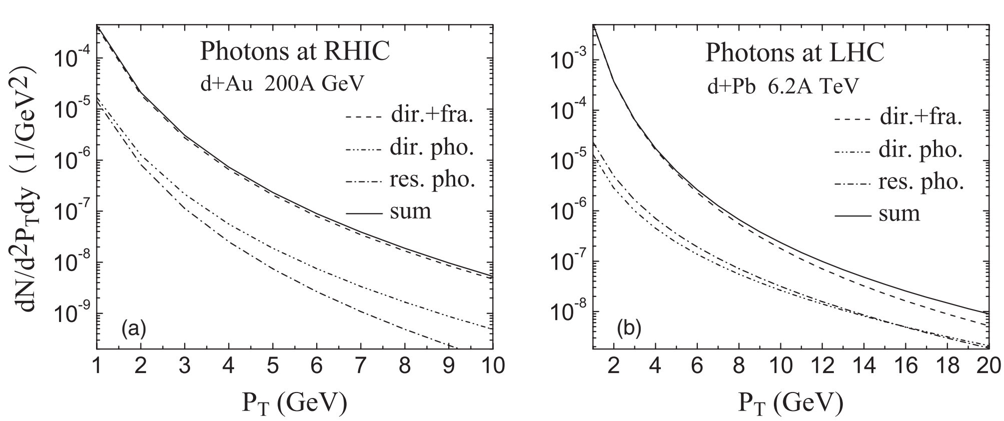

FIG. 7. Same as Fig. 2 but for the real photon production in central d + Au collisions at RHIC (a) and d + Pb collisions at LHC (b).

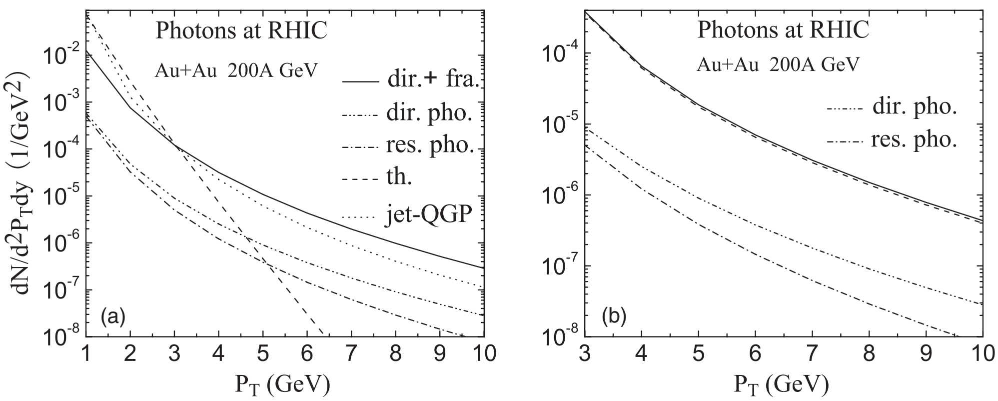

FIG. 8. Same as Fig. 3 but for the real photon production in central Au + Au collisions at RHIC energies.

The yield of jets produced by AA collisions can be written as

$$\frac{dN_{\rm jet}}{d^2P_T'dy} = T_{AA}E'\frac{d\sigma_{\rm jet}}{d^3P'}(y=0), \tag{17}$$

where the nuclear thickness T_{AA} for zero impact parameter is $9A^2/8\pi R_\perp^2$. The invariant cross section of the jet production is given by

$$E'\frac{d\sigma_{\rm jet}}{d^3P'} = \frac{1}{\pi}\int dx_a G_{a/A}(x_a,Q^2)G_{b/B}(x_b,Q^2)\frac{x_a x_b}{x_a - x_1} \times \frac{d\hat{\sigma}_{\rm par.}}{d\hat{t}}(x_a,x_b,P_T'). \tag{18}$$

Jets passing through the QGP will lose energy. Induced gluon bremsstrahlung, rather than elastic scattering of partons, is the dominant mechanism of the jet energy loss [3,27,28,40,41]. Based on the AMY formulism, the energy loss of the final state partons can be described as a dependence of the final state parton spectrum $dN_{\rm jet}/dE$ on time [3,42]. Besides, the energy loss of jets can be scaled as the square of the distance traveled through the medium [43]. Jets travel only a short distance through the plasma before the jet-photon (or virtual photon) conversion, and do not lose a significant amount of energy. The energy loss effect of jets before they convert into photons (or virtual photons) is found to be small, about 20% [3,27,28].

The rate of the photon production by Compton scattering and annihilation of jets in the hot medium can be written as [27,28]

$$E\frac{dR_{{\rm jet}-\gamma}}{d^3P} = \frac{\alpha\alpha_s e_q^2}{4\pi^2}f_{\rm jet}(\boldsymbol{p}_\gamma)T^2\left[2\ln\left(\frac{6E_\gamma}{\pi\alpha_s T}\right)+C\right], \tag{19}$$

where the constant is $C = C_{\rm Com.} + C_{\rm ann.}$. The detailed processes of the thermal contribution and jet-γ (γ^*) conversion are discussed in Refs. [29,30]. We briefly review the contribution of thermal photons and dileptons. The Landau-Pomeranchuk-Migdal (LPM) effect for the thermal production and jet-γ (γ^*) conversion [29,30] is not considered in our paper. In the calculation we use the Bjorken 1+1-D evolution, the authors of Refs. [29,30] consider the transverse expansion of the hot and dense matter (3+1-D) in the thermal photon and dilepton production.

V. NUMERICAL RESULTS

The yield of large P_T dileptons in a mass range between $M_{\rm min}$ and $M_{\rm max}$ can be defined as [4,5]

$$\frac{dN_{AB\to l^+l^-X}}{d^2P_Tdy} = \int_{M_{\rm min}}^{M_{\rm max}}\frac{2M}{\pi}\frac{dN_{AB\to l^+l^-X}}{dM^2dP_T^2dy}dM, \tag{20}$$

in this paper we choose the range 100 MeV$\leqslant M \leqslant$300 MeV.

The results of our calculation for AA collisions in the minimum bias case are plotted. In Figs. 1 and 2 we plot the contribution of dileptons produced by direct and resolved photoproduction processes for pp and dA collisions at RHIC and

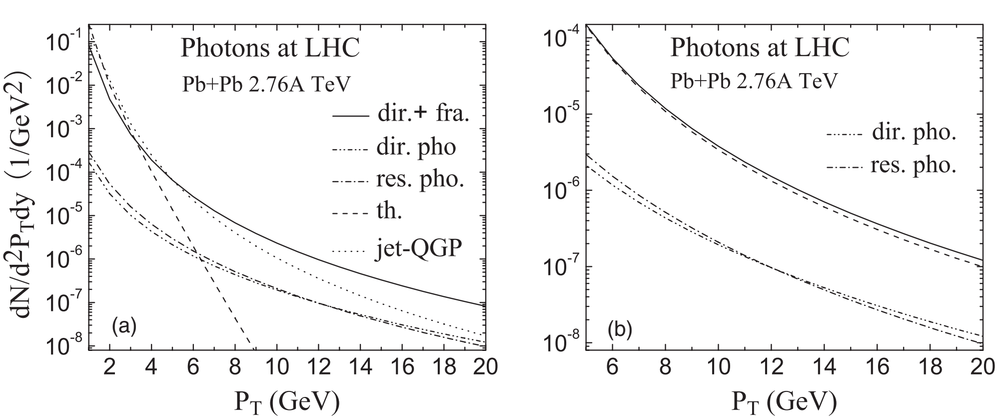

FIG. 9. Same as Fig. 4 but for the real photon production in central Pb + Pb collisions at $\sqrt{s_{NN}} = 2.76$ TeV.

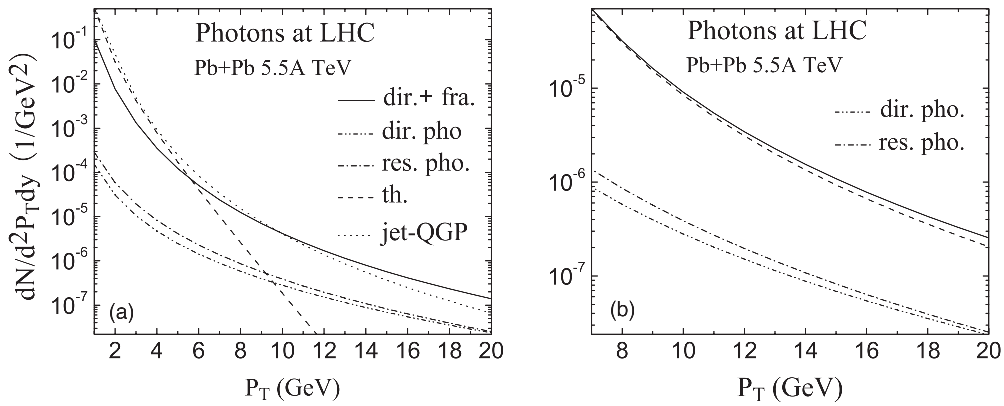

FIG. 10. Same as Fig. 5 but for the real photon production in central Pb + Pb collisions at $\sqrt{s_{NN}} = 5.5$ TeV.

LHC energies. In panel (a) of Figs. 1 and 2 the dilepton spectra of direct and resolved photoproduction processes (dash-dot line and dash-dot-dot line) are compared with the spectrum of direct and fragmentation dileptons (dashed line) for $p + p$ collisions and $d +$ Au collisions at RHIC, respectively. We find that the contribution of photoproduction processes is not prominent for $p + p$ and $d +$ Au collisions at RHIC energies. However, photoproduction processes start playing an interesting role for $p + p$ collisions and $d +$ Pb collisions at LHC. The contribution of photoproduction processes is evident in the region of $P_T > 1$ GeV for $p + p$ collisions [Fig. 1(b)], and $P_T > 1$ GeV for $d +$ Pb collisions at LHC energies [Fig. 2(b)].

In panel (a) of Fig. 3 we plot the results for direct dileptons (dir.), fragmentation dileptons (fra.), the jet-dilepton conversion (jet-QGP) in the thermal plasma, and thermal dileptons (th.) produced by the QGP in Au + Au collisions at RHIC. The dilepton spectra of direct (dir. pho.) and resolved photoproduction processes (res. pho.) are also plotted. The results for Pb + Pb collisions at $\sqrt{s_{NN}} = 2.76$ TeV and 5.5 TeV are shown in Figs. 4(a) and 5(a), respectively. In Fig. 3(b) we see that the contribution of photoproduction processes is still weak for Au + Au collisions at RHIC. However, the contribution of photoproduction processes becomes evident in the large P_T region at LHC energies. In Figs. 4(b) and 5(b) the spectra of dileptons produced by direct and resolved photoproduction processes (dash-dot line and dash-dot-dot line) are compared with the spectrum of direct dileptons, fragmentation dileptons, thermal dileptons, and the jet-dilepton conversion (dashed line), we find that the contribution of dileptons produced by photoproduction processes is evident in the region of $P_T > 2$ GeV for Pb + Pb collisions at $\sqrt{s_{NN}} = 2.76$ TeV, and $P_T > 4$ GeV for Pb + Pb collisions at $\sqrt{s_{NN}} = 5.5$ TeV.

The contribution of real photons produced by direct and resolved photoproduction processes is also negligible for pp, dA, and AA collisions at RHIC energies [Figs. 6(a), 7(a), and 8]. However, the contribution of photoproduction processes is evident in the region of $P_T > 4$ GeV for $p + p$ collisions at $\sqrt{s} = 7$ TeV [Fig. 6(b)], $P_T > 4$ GeV for $d +$ Pb collisions at $\sqrt{s_{NN}} = 6.2$ TeV [Fig. 7(b)], $P_T > 5$ GeV for Pb + Pb collisions at $\sqrt{s_{NN}} = 2.76$ TeV [Fig. 9(b)], and $P_T > 7$ GeV for Pb + Pb collisions at $\sqrt{s_{NN}} = 5.5$ TeV [Fig. 10(b)].

The photon spectrum $f_{\gamma/q}$ from the charged parton depends on the collision energy $\sqrt{s_{NN}}$. We express the photon spectrum as $f_{\gamma/q} \propto \ln[(\hat{s}/4 - m_l^2)/1\,\text{GeV}^2] = \ln(s_{NN}/1\,\text{GeV}^2) + \ln(x_a x_b z_a \ldots/4 - m_l^2/s_{NN})$, where $\hat{s} = x_a x_b z_a s_{NN}$ for direct photoproduction processes and $\hat{s} = x_a x_b z_a z_{a'} s_{NN}$ for resolved photoproduction processes. Since the collision energy at LHC is larger than the collision energy at RHIC($s_{NN}^{\text{LHC}} \gg s_{NN}^{\text{RHIC}}$), the photon spectrum becomes important at LHC energies. Therefore the contribution of photoproduction processes is evident at LHC.

We also plot the spectra of thermal dileptons and photons, because the contribution of the thermal information is dominant in the small P_T region. We show the results of the jet-dilepton (photon) conversion taking into account an effective 20% energy loss of jets before conversion into dileptons (photons) [3,28]. The spectra of the jet-dilepton conversion fall off with the transverse momentum of dileptons faster than the spectrum of primary hard dileptons due to the attenuation function $\exp(-P_T^2/4P_T^{\prime\text{jet}}T)$ in Eq. (15) [Figs. 3(a), 4(a), and 5(a)]. Since the rate of the jet-photon conversion is $R_{\text{jet}-\gamma} \propto f_{\text{jet}}$, the spectra of the jet-photon conversion do not drop quickly with the transverse momentum [Figs. 8(a), 9(a), and 10(a)].

VI. SUMMARY

We investigate the production of large P_T dileptons and photons in relativistic pp, dA, and AA collisions by direct and resolved photoproduction processes. In the initial parton scattering the charged parton of the incident nucleon can emit large P_T photons, then the high energy photons interact with the partons of another incident nucleon by the QED Compton scattering. Furthermore, the hadron-like photons also can interact with the partons of the nucleon by the annihilation and Compton scattering. The numerical results indicate that the contribution of photoproduction processes is negligible for pp, dA, and AA collisions at RHIC energies, but the contribution becomes evident at LHC energies.

ACKNOWLEDGMENTS

This work is supported by the National Natural Science Foundation of China under Grants No. 10665003 and No. 11065010.

[1] J. F. Owens, Rev. Mod. Phys. **59**, 465 (1987).
[2] R. D. Field, *Applications of Perturbative QCD* (Addison-Wesley Publishing Company, Reading, MA, 1989).
[3] S. Turbide, C. Gale, S. Jeon, and G. D. Moore, Phys. Rev. C **72**, 014906 (2005).
[4] Z. B. Kang, J. W. Oiu, and W. Vogelsang, Phys. Rev. D **79**, 054007 (2009).
[5] Z. Kang, J. W. Oiu, and W. Vogelsang, Nucl. Phys. A **830**, 571 (2009).
[6] E. L. Berger, J. Oiu, and X. Zhang, Phys. Rev. D **65**, 034006 (2002).
[7] X. N. Wang, Phys. Lett. B **595**, 165 (2004).
[8] M. Glück, E. Reya, and A. Vogt, Z. Phys. C **53**, 127 (1992).
[9] J. W. Qiu, Nucl. Phys. B **291**, 746 (1987).
[10] M. Glück, E. Reya, and A. Vogt, Phys. Rev. D **46**, 1973 (1992).
[11] K. J. Eskola, V. J. Kolhinen, and C. A. Salgado, Eur. Phys. J. C **9**, 61 (1999); K. J. Eskola, V. J. Kolhinen, and P. V. Ruuskanen, Nucl. Phys. B **535**, 351 (1998).
[12] K. Kajantie, J. Kapusta, L. McLerran, and A. Mekjian, Phys. Rev. D **34**, 2746 (1986).
[13] J. Kapusta, P. Lichard, and D. Seibert, Phys. Rev. D **44**, 2774 (1991).
[14] J. D. Bjorken, Phys. Rev. D **27**, 140 (1983).
[15] C. Y. Wong, *Introduction to High Energy Heavy-Ion Collisions* (World Scientific, Singapore, 1994).
[16] E. Shuryak and L. Xiong, Phys. Rev. Lett. **70**, 2241 (1993).
[17] R. D. Pisarski, Phys. Lett. B **110**, 155 (1982).
[18] E. V. Shuryak and I. Zahed, Phys. Rev. C **70**, 021901(R) (2004).
[19] R. Rapp and E. Shuryak, Phys. Lett. B **473**, 13 (2000).
[20] C. Spieles *et al*., Eur. Phys. J. C **5**, 349 (1998).
[21] Jan-e Alam, D. K. Srivastava, B. Sinha, and D. N. Basu, Phys. Rev. D **48**, 1117 (1993).
[22] J. K. Nayak, J. Alam, S. Sarkar, and B. Sinha, Phys. Rev. C **78**, 034903 (2008).
[23] T. Peitzmann and M. H. Thoma, Phys. Rep. **364**, 175 (2002).
[24] S. Turbide, R. Rapp, and C. Gale, Phys. Rev. C **69**, 014903 (2004).
[25] E. L. Bratkovskaya and W. Cassing, Nucl. Phys. A **619**, 413 (1997).
[26] C. M. Hung and E. V. Shuryak, Phys. Rev. C **56**, 453 (1997).
[27] R. J. Fries, B. Müller, and D. K. Srivastava, Phys. Rev. Lett. **90**, 132301 (2003).
[28] R. J. Fries, B. Müller, and D. K. Srivastava, Phys. Rev. C **72**, 041902(R) (2005).
[29] S. Turbide, C. Gale, E. Frodermann, and U. Heinz, Phys. Rev. C **77**, 024909 (2008).
[30] F. M. Liu, T. Hirano, K. Werner, and Y. Zhu, Phys. Rev. C **79**, 014905 (2009).
[31] L. G. Landsberg, Phys. Rep. **128**, 301 (1985).
[32] R. Nisius, Phys. Rep. **332**, 165 (2000).
[33] M. Krawczyk, A. Zembrzuski, and M. Staszel, Phys. Rep. **345**, 265 (2001).
[34] J. R. Forshaw, arXiv:hep-ph/9706319.
[35] Y. D. Li and L. S. Liu, Phys. Lett. B **377**, 177 (1996).
[36] G. Baur, K. Hencken, and D. Trautmann, J. Phys. G **24**, 1657 (1998).
[37] M. Drees, R. M. Godbole, M. Nowakowski, and S. D. Rindani, Phys. Rev. D **50**, 2335 (1994).
[38] D. K. Srivastava, C. Gale, and R. J. Fries, Phys. Rev. C **67**, 034903 (2003).
[39] Y. P. Fu and Y. D. Li, Chin. Phys. Lett. **27**, 101202 (2010); Nucl. Phys. A **865**, 76 (2011).
[40] M. Gyulassy and M. Plümer, Phys. Lett. B **243**, 432 (1990).
[41] X. N. Wang, M. Gyulassy, and M. Plümer, Phys. Rev. D **51**, 3436 (1995).
[42] P. Arnold, G. D. Moore, and L. Yaffe, J. High Energy Phys. 11 (2001) 057.
[43] R. Baier *et al*., Nucl. Phys. B **484**, 265 (1997).